

Supplementary material to:

Multi-center and multi-vendor validation study across 1.5T and 3T scanners (part 1): apparent diffusion coefficient standardization in a diffusion MRI phantom

Table of contents:

Figure S1: Phantom positioning for coronal (a), axial (b) and sagittal (c) imaging plane acquisitions.

Figure S2: Example of SNR and image quality analysis for Scanner 8 along coronal plane

Figure S3: Bias% between pure water vial (PVP = 0%) in the isocenter and in the inner/outer circle. The region shaded in red represents the 3% range. In the table below, bias mean values and limits of agreement are reported for each imaging plane and field strength.

Figure S4: Vials positioning (a) and example of sigmoidal (in orange) and power law (blue) fit for temperature determination. For each fit the estimated temperature and error are reported.

Fig. S5: Linear fit obtained by plotting the $\log(\text{ADC})$ as a function of the inverse of the temperature for each PVP concentration (a). Example of temperature rescaling (b). Error% on ADC after temperature rescaling as a function of the phantom temperature, the ADC measurement error from the fit and assuming a temperature error of 1°C (c).

Table S1: SNR from difference method for each vial and scanner

Table S2: SNR from multiple acquisitions method for each vial and scanner

Table S3: Temperature adjusted measured ADC values

Table S4: Accuracy error% for each vial and scanner

Table S5: Intra-session coefficient of variation ($CV_{\text{intra}}\%$) for each vial and scanner

Fig. S6: GLMM results for accuracy error (in %) compared across slice orientations in the full range (a) and reduced range (b)

Fig. S7: Results of GLMM in the reduced range on accuracy error (a), repeatability (b) and precision error (c) across all imaging planes. Accuracy error is also reported for average values (d). All results are reported as least-square means and standard errors.

Table S5: Summary of GLMM statistical significance of predictors for accuracy, repeatability and precision. Field and vendor were tested as independent predictors and through their interaction for each variable.

Table S6: Intra-session coefficient of variation ($CV_{\text{intra}}\%$) for each vial and scanner

Figure S8: GLMM results for intra-session coefficient of variation ($CV_{\text{intra}}\%$) compared across slice orientations in the full range (a) and reduced range (b). Horizontal lines represent the paired comparisons with their relative Bonferroni-corrected significance value (ns = $p > 0.05$, * = $p < 0.05$, ** $p < 0.01$, *** = $p < 0.001$).

Figure S9: Bland Altman plots for test-retest measurements across each imaging slice orientation

Figure S10: GLMM results for precision error% compared across slice orientations in the full range (a) and reduced range (b). Horizontal lines represent the paired comparisons with their relative Bonferroni-corrected significance value (ns = $p > 0.05$, * = $p < 0.05$, ** $p < 0.01$, *** = $p < 0.001$).

Table S7: Results of ADC variance contributions, ICC_{intra} and ICC_{inter} are reported for both field strengths

Figure S1: Phantom positioning for coronal (a), axial (b) and sagittal (c) imaging plane acquisitions.

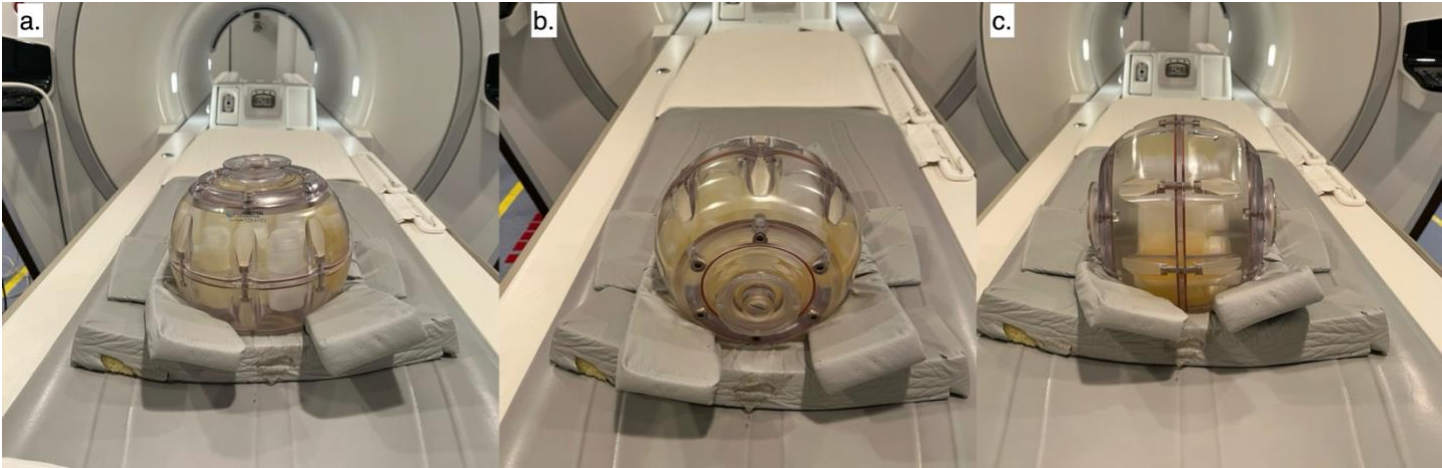


Figure S2: Example of SNR and image quality analysis for Scanner 8 along coronal plane

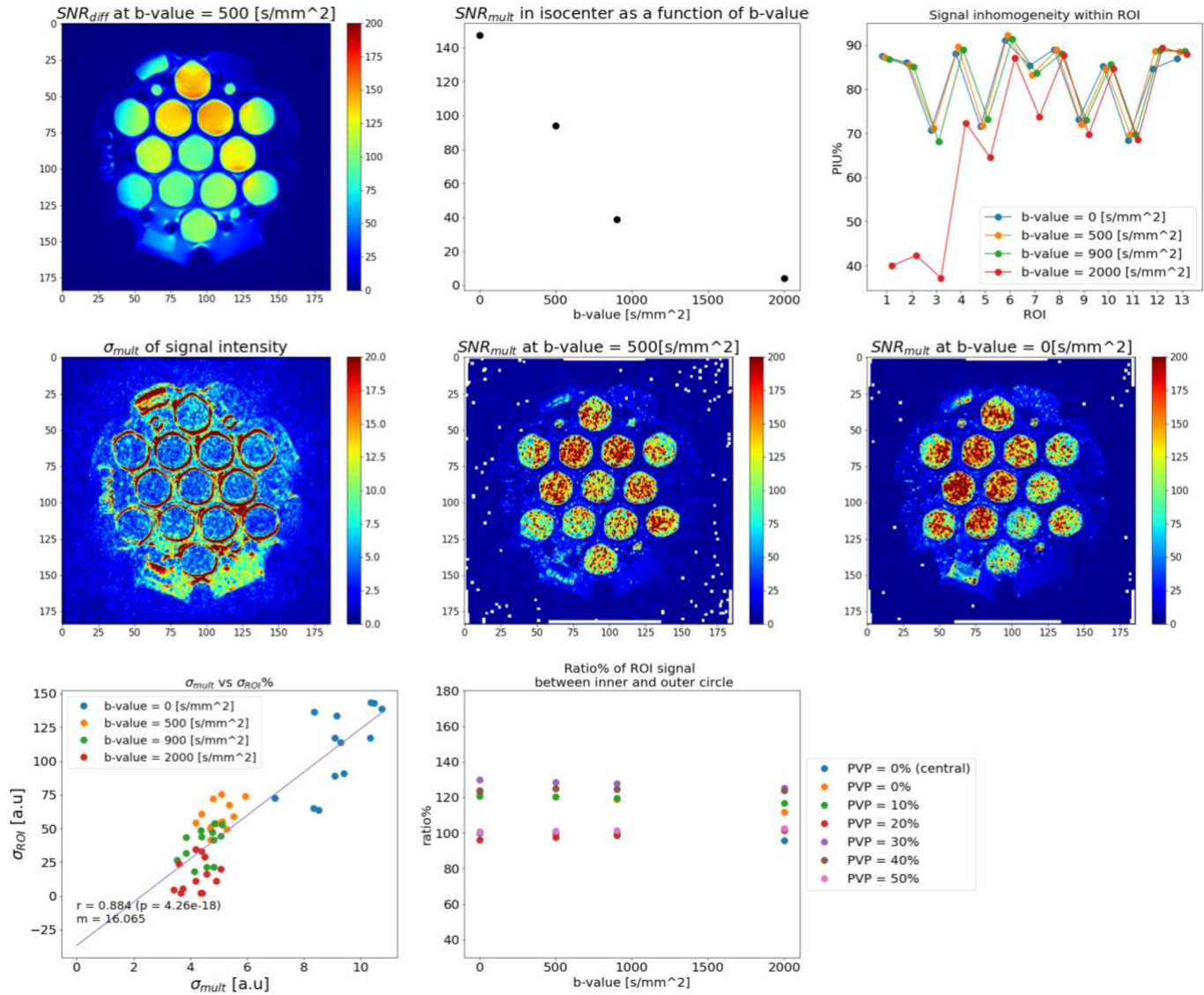
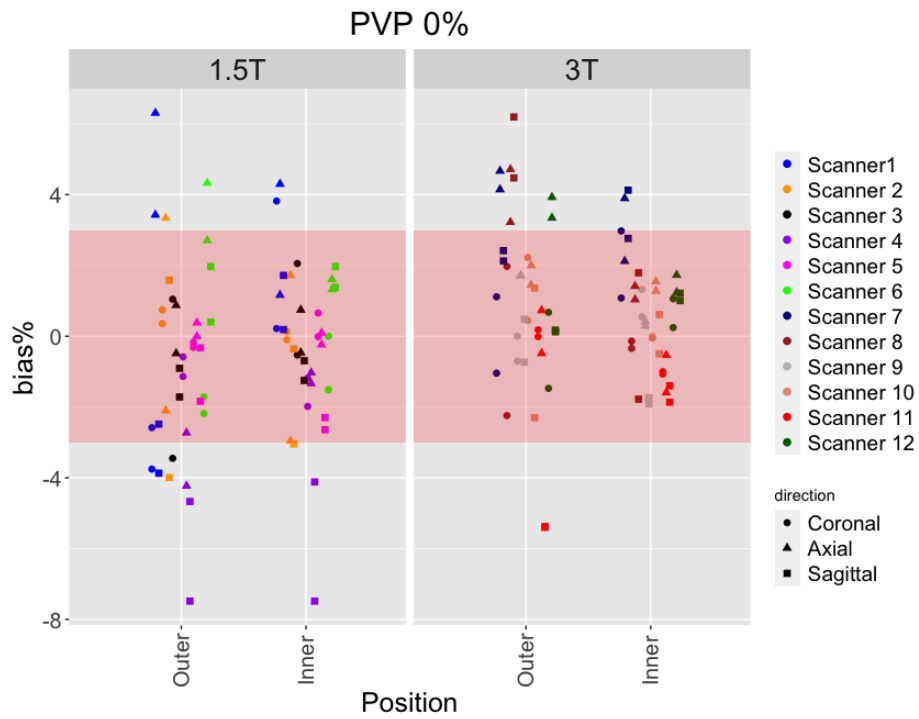


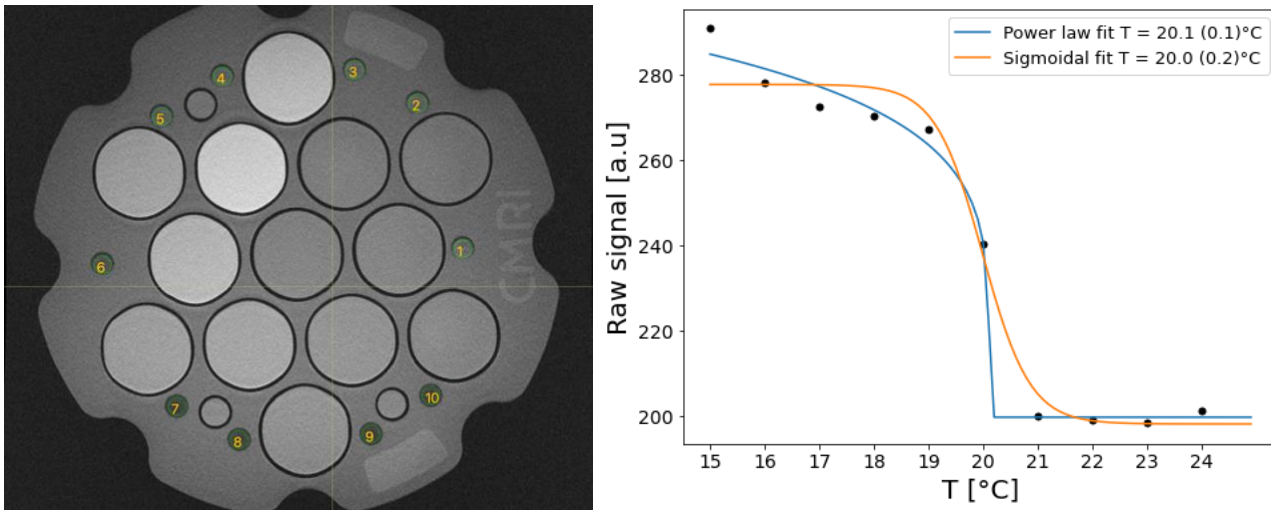
Figure S3: Bias% between pure water vial (PVP = 0%) in the isocenter and in the inner/outer circle. The region shaded in red represents the 3% range. In the table below, bias mean values and limits of agreement are reported for each imaging plane and field strength.



	<i>1.5T</i>		<i>3T</i>	
	Inner (~4cm)	Outer (~8cm)	Inner (~4cm)	Outer (~8cm)
<i>Coronal [%]</i>	0.13 (-2.94, 3.20)	-1.14 (-4.28, 1.99)	0.39 (-1.80, 2.58)	0.10 (-2.51, 2.70)
<i>Axial [%]</i>	0.41 (-3.21, 4.03)	0.98 (-5.15, 7.12)	1.07 (-1.62, 3.75)	2.59 (-0.64, 5.84)
<i>Sagittal [%]</i>	-1.39 (-6.75, 3.98)	-1.94 (-7.34, 3.45)	0.19 (-3.81, 4.19)	0.30 (-6.54, 7.13)

Example of temperature determination

Figure S4: Vials positioning (a) and example of sigmoidal (in orange) and power law (blue) fit for temperature determination. For each fit the estimated temperature and error are reported.



In order to estimate the phantom temperature, ordered circular ROIs (5.5 mm of diameter) were placed over the LC MR-readable thermometer vials as reported in Figure a.

For each ROI, the average signal undergoes a transition from dark to bright at a vial specific temperature. The phantom temperature T_C is then found in the range between the highest transition temperature of the vials in a bright state and the lowest of those in a dark state.

To determine the phantom temperature a four-parameters sigmoidal fit given by $S(T) = A \frac{1}{1+e^{\gamma(T-T_C)}} + B$ was used. T_C estimates the system temperature, A the amplitude in signal intensity from a dark to a bright state, γ the slope of the transition and B the offset defined by the dark state signal. In this case we assume a two-state transition from a bright to a dark state.

An alternative fit, proposed in PhantomViewer, uses a four-parameter power law model to estimate the transition temperature $S(T) = A \cdot (T_C - T)^\gamma + B$. In this case we assume that the signal is proportional to the order parameter plus a constant offset and the order parameter goes to zero as the temperature increase as $(T_C - T)^\gamma$.

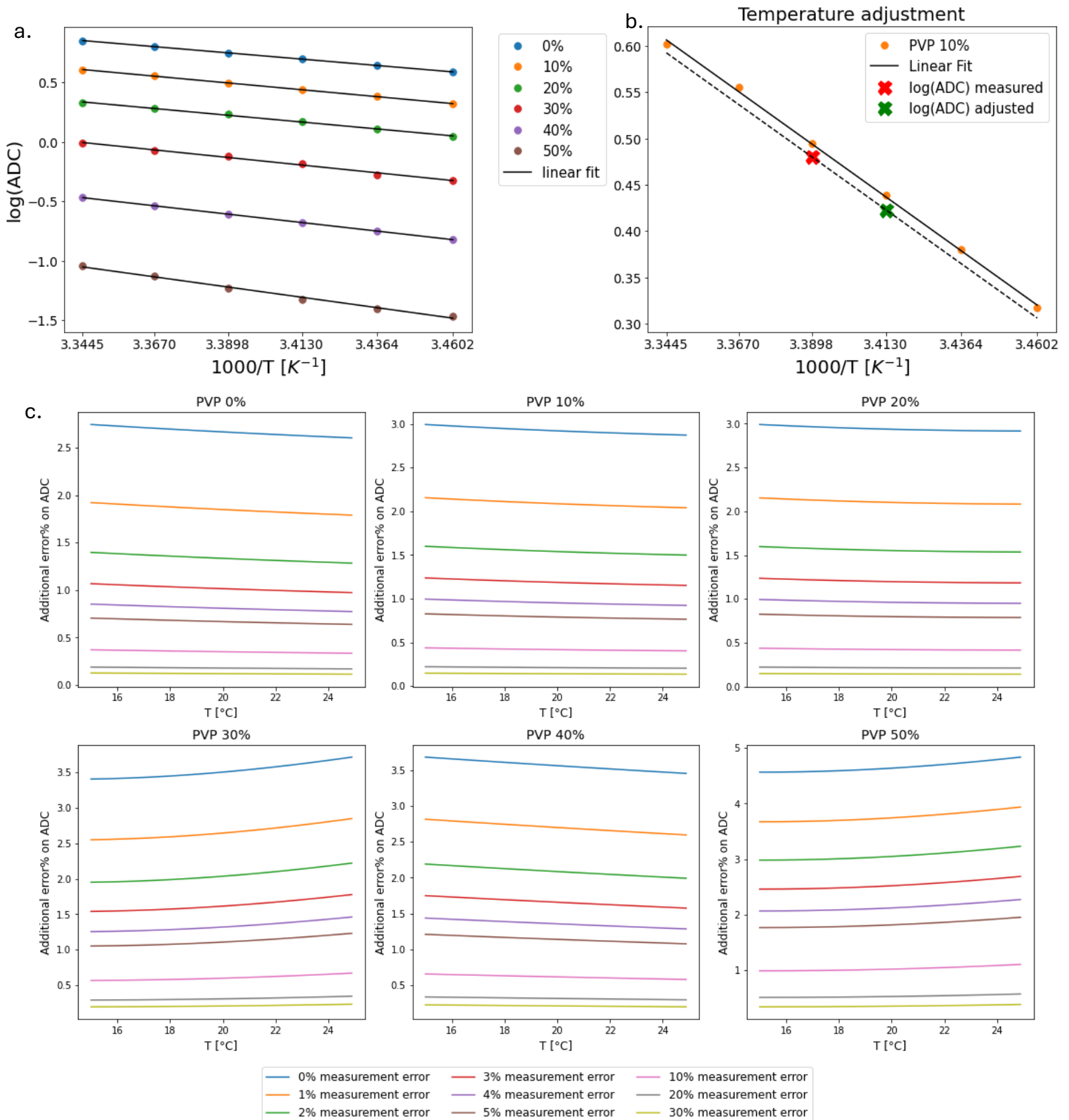
Here reported are the measured temperatures obtained with both fits

<i>Scanner</i>	<i>Sigmoidal fit</i>	<i>Power law fit</i>
1	20.5 ± 0.2	20.0 ± 0
2	24.0*	24.0*
3	20.0 ± 0.4	20.0 ± 0
4	20.7 ± 0.5	20.0 ± 0
5	20.5 ± 0.6	20.0 ± 0
6	20.1 ± 0.5	20.0 ± 0
7	20.6 ± 0.5	21.0 ± 1
8	22.0 ± 0.4	22.3 ± 0
9	21.8 ± 0.5	22.0 ± 0
10	20.0 ± 0.2	20.1 ± 0.1
11	20.6 ± 0.6	21.0 ± 0
12	20.6 ± 0.5	21.0 ± 0

*all vials had transitioned to a bright state

Example of temperature adjustment

Figure S5: Linear fit obtained by plotting the $\log(\text{ADC})$ as a function of the inverse of the temperature for each PVP concentration (a). Example of temperature rescaling (b). Error% on ADC after temperature rescaling as a function of the phantom temperature, the ADC measurement error from the fit and assuming a temperature error of 1°C (c).



The rescaling was performed as a two-step process.

1. The temperature dependence of ADC values is fit by Arrhenius model as described by Amouzandeh et al. (DOI: 10.1002/mp.15556) with a linear regression model

$$ADC = A \cdot e^{-\frac{E_a}{RT}} \Rightarrow \log(ADC) = c_1 + c_2 \cdot \frac{1000}{T} \Rightarrow y = c_1 + c_2 \cdot x_T$$

Linear fits are obtained from reference values provided by the phantom manufacturer are shown in Figure S3a.

The coefficients c_1 and c_2 were then estimated for each PVP concentration.

PVP	c_1	c_2
0%	8.45 ± 0.09	-2.27 ± 0.03
10%	8.88 ± 0.13	-2.48 ± 0.04
20%	8.58 ± 0.17	-2.47 ± 0.05
30%	9.24 ± 0.39	-2.76 ± 0.05
40%	9.74 ± 0.06	-3.05 ± 0.02
50%	11.39 ± 0.46	-3.72 ± 0.14

2. For each PVP vial the same linear fit was used to rescale each value

$$y_{rescaled} = y_{measured} + c_2 \cdot (x_{20} - x_{Tmeasured})$$

This is shown in Figure S2b where measured $\log(ADC)$ (shown in red) is rescaled to 20 °C (shown in green).

Based on this rescaling we estimated that assuming a maximum error on temperature estimation of 1°C corresponding to the resolution of the LC thermometer, the error on ADC measurement would be on average an additional 2-3% (up to 5% only for PVP = 50%) compared to measurement error that comes from fitting the mono-exponential model (Figure S3c).

Table S1: SNR from difference method for each vial and scanner

SNR _{diff} 1.5T																		
ROI	Scanner 1			Scanner 2			Scanner 3			Scanner 4			Scanner 5			Scanner 6		
	Cor	Ax	Sag	Cor	Ax	Sag	Cor	Ax	Sag	Cor	Ax	Sag	Cor	Ax	Sag	Cor	Ax	Sag
1	26.7	26.1	23.9	47.1	39.2	37.5	42.4	40.3	40.3	46.4	45.6	45.2	89.3	68.7	77.7	178.6	147.0	186.1
2	27.9	23.6	20.0	49.6	50.3	49.0	45.5	50.8	48.6	46.9	52.5	48.5	87.8	73.5	76.3	176.0	140.7	186.7
3	28.1	19.1	17.1	55.1	58.5	52.7	39.7	87.1	83.1	46.8	66.1	66.7	88.7	70.7	75.3	157.3	135.4	173.6
4	26.8	19.8	22.0	50.4	39.8	36.0	39.4	59.2	59.0	43.3	38.8	43.1	83.6	63.8	73.3	159.4	133.4	169.5
5	27.2	19.7	28.2	51.7	45.7	37.5	38.6	81.0	73.7	43.1	42.2	42.1	83.1	57.7	73.3	146.9	129.0	158.6
6	24.3	20.6	27.9	42.7	40.7	37.2	38.3	45.1	37.9	39.0	40.1	41.3	74.1	54.0	67.5	144.5	121.2	156.0
7	25.6	24.3	42.5	40.3	65.8	60.4	42.2	42.8	27.4	37.9	61.5	67.5	71.3	50.5	68.2	138.7	114.4	160.7
8	20.1	22.8	25.8	36.5	36.8	36.9	33.3	28.2	25.4	33.5	43.0	45.9	63.6	47.8	57.7	125.7	108.3	137.5
9	20.0	33.5	28.2	38.5	37.4	38.1	31.8	28.9	26.0	31.5	59.6	64.6	57.5	45.1	55.6	115.1	112.6	128.3
10	13.7	19.1	12.8	30.9	25.4	24.5	26.6	22.3	21.3	27.1	27.2	35.8	51.5	40.6	46.5	105.1	95.6	111.8
11	14.1	25.9	8.9	31.1	31.8	24.7	28.5	24.8	23.4	25.7	24.4	26.7	48.6	42.3	44.5	98.2	97.1	103.5
12	5.1	7.0	3.6	22.4	22.5	21.6	20.9	16.3	15.4	19.6	19.9	16.8	36.8	32.1	32.6	81.6	69.4	86.9
13	5.1	5.8	3.3	21.9	36.9	36.0	24.1	21.3	18.1	19.3	26.4	23.0	37.5	36.2	30.8	79.6	63.4	90.2
SNR _{diff} 3T																		
ROI	Scanner 7			Scanner 8			Scanner 9			Scanner 10			Scanner 11			Scanner 12		
	Cor	Ax	Sag	Cor	Ax	Sag	Cor	Ax	Sag	Cor	Ax	Sag	Cor	Ax	Sag	Cor	Ax	Sag
1	151.9	114.2	122.6	147.3	90.6	87.2	100.8	114.7	88.6	120.0	139.9	62.0	117.8	91.0	89.2	NA	NA	NA
2	144.9	115.5	139.8	146.9	91.5	86.6	100.6	119.8	92.6	116.2	131.2	56.8	123.5	102.5	95.5	NA	NA	NA
3	109.6	125.9	124.5	119.2	116.9	106.6	90.5	116.0	80.7	114.5	129.1	50.7	104.6	96.0	78.0	NA	NA	NA
4	136.2	127.7	109.3	140.0	91.8	85.6	100.2	117.7	89.7	115.6	139.5	56.2	111.8	88.6	86.2	NA	NA	NA
5	110.8	135.2	87.6	115.7	92.1	73.3	86.5	123.1	77.5	122.8	170.3	66.5	101.4	86.1	77.3	NA	NA	NA
6	128.9	96.2	110.1	137.1	81.4	75.4	93.8	106.8	77.4	113.0	145.0	63.8	105.0	84.5	74.6	NA	NA	NA
7	114.0	74.1	122.6	142.2	85.8	66.5	90.2	99.4	60.7	103.6	217.6	107.2	79.9	90.7	88.9	NA	NA	NA
8	114.3	81.8	100.0	120.5	81.1	83.6	82.3	91.8	65.5	98.5	124.6	65.4	93.1	74.0	70.2	NA	NA	NA
9	88.4	100.6	77.0	92.5	111.0	119.5	62.2	83.7	56.6	89.9	129.2	75.8	91.0	68.2	63.9	NA	NA	NA
10	90.0	75.6	73.9	91.3	76.0	74.3	65.5	77.4	53.4	74.0	89.0	45.3	80.6	59.7	57.2	NA	NA	NA
11	63.9	77.3	61.1	73.8	86.6	61.6	49.7	68.8	47.9	63.6	71.8	36.2	73.7	57.9	46.6	NA	NA	NA

12	65.3	53.4	61.9	67.1	45.8	39.7	45.9	55.7	38.7	49.6	59.7	25.4	58.3	48.0	43.7	NA	NA	NA
13	54.5	42.5	75.2	66.7	39.8	27.0	45.5	52.0	30.8	45.2	64.3	26.9	40.3	46.0	45.7	NA	NA	NA

SNR = Signal to noise ratio; Cor = coronal; Ax = axial; Sag = sagittal

Table S2: SNR from multiple acquisitions method for each vial and scanner

SNR _{mult} 1.5T																		
Scanner 1			Scanner 2			Scanner 3			Scanner 4			Scanner 5			Scanner 6			
ROI	Cor	Ax	Sag	Cor	Ax	Sag	Cor	Ax	Sag	Cor	Ax	Sag	Cor	Ax	Sag	Cor	Ax	Sag
1	32.2	27.3	27.1	61.1	50.3	48.0	52.9	53.0	50.6	61.1	53.7	78.2	105.5	109.4	83.7	144.9	146.1	148.6
2	35.3	27.3	29.1	70.8	66.5	71.2	59.3	72.7	63.9	63.5	72.5	119.6	98.4	69.4	82.3	162.8	143.0	137.5
3	26.4	19.7	25.7	83.1	88.3	82.8	58.6	142.6	111.7	62.4	74.8	188.3	93.4	47.5	100.1	164.3	163.4	160.7
4	29.2	23.1	31.4	66.3	55.5	53.7	53.9	85.1	83.9	70.8	50.9	108.3	89.6	79.7	79.8	173.6	171.5	130.4
5	24.7	19.3	37.7	73.4	84.8	71.9	48.3	112.0	106.9	71.6	50.2	97.2	89.0	67.2	84.0	140.8	194.0	137.2
6	34.9	23.3	44.5	59.5	60.2	57.0	48.4	59.1	55.3	61.4	53.2	87.8	83.6	53.8	63.1	147.1	139.3	137.3
7	30.2	16.6	54.3	55.9	85.1	86.6	53.8	59.5	46.7	49.4	84.0	86.8	79.9	75.5	101.4	136.9	143.8	143.0
8	33.4	22.6	32.0	49.7	56.8	56.6	41.7	36.8	32.7	44.1	62.6	94.5	71.6	62.8	44.8	138.4	131.2	122.9
9	24.0	20.5	39.2	53.9	65.4	61.9	45.5	40.4	42.0	45.6	97.8	110.0	59.1	73.8	79.9	121.9	104.3	115.6
10	17.3	18.0	17.5	39.9	37.8	37.2	38.7	31.2	24.2	42.7	36.9	50.7	59.2	68.3	59.0	104.0	106.8	108.6
11	19.6	25.6	13.2	44.3	49.6	46.4	41.3	41.4	33.4	44.0	36.0	55.0	56.2	45.8	63.8	107.1	94.0	112.9
12	7.7	10.2	5.7	31.8	30.4	31.0	30.2	21.8	21.0	28.0	25.5	36.8	44.8	32.6	46.1	90.0	73.0	109.4
13	8.4	7.7	5.3	36.1	50.3	49.9	36.2	34.6	26.8	32.6	47.7	49.2	52.1	30.9	48.6	108.5	75.8	147.2
SNR _{mult} 3T																		
Scanner 7			Scanner 8			Scanner 9			Scanner 10			Scanner 11			Scanner 12			
1	132.3	128.8	145.8	141.9	105.5	107.2	116.3	126.3	115.2	98.7	83.6	91.1	154.1	92.5	108.8	NA	NA	NA
2	119.7	110.4	217.8	140.0	122.8	157.2	121.9	178.1	175.4	131.8	73.0	57.0	167.5	145.5	110.6	NA	NA	NA
3	79.3	92.2	142.5	115.6	158.3	176.1	125.2	148.2	217.2	133.5	51.8	62.7	136.2	134.5	104.0	NA	NA	NA
4	130.4	121.1	117.0	167.4	131.5	150.1	137.5	141.6	168.0	113.3	77.6	57.0	125.8	144.7	97.3	NA	NA	NA
5	109.8	107.4	99.1	124.9	152.0	143.1	138.5	119.3	185.3	145.9	66.2	52.6	120.4	144.3	134.7	NA	NA	NA
6	134.3	133.8	148.9	149.7	123.7	131.2	116.4	97.7	131.6	131.8	113.5	50.9	133.1	136.7	83.0	NA	NA	NA
7	106.3	78.6	158.5	132.5	167.7	113.4	116.2	99.4	117.2	156.7	90.2	68.7	120.2	139.4	102.2	NA	NA	NA

8	109.3	74.5	130.5	132.4	116.4	108.0	101.9	84.1	89.5	132.9	107.5	44.8	130.5	82.6	89.2	NA	NA	NA
9	87.6	61.9	101.5	98.6	166.3	131.0	109.6	69.3	70.5	128.0	116.3	57.9	118.1	71.2	105.4	NA	NA	NA
10	91.4	85.0	89.7	100.4	76.5	96.3	86.7	75.6	64.8	108.0	123.5	79.8	96.8	56.8	89.6	NA	NA	NA
11	77.5	70.6	79.5	105.7	133.2	100.4	92.8	85.2	75.6	95.6	99.6	55.4	103.0	60.2	84.7	NA	NA	NA
12	70.9	62.3	88.3	80.4	75.5	81.2	65.9	75.6	69.9	79.8	95.9	36.6	87.3	61.8	56.4	NA	NA	NA
13	67.0	49.7	124.6	77.9	85.1	73.9	61.6	92.9	81.9	84.8	113.3	58.5	68.4	68.5	49.2	NA	NA	NA

SNR = Signal to noise ratio; Cor = coronal; Ax = axial; Sag = sagittal

Table S3: Temperature adjusted measured ADC values

1.5 T ADC x 10⁻³ [mm²/s]

ROI	Ref	Scanner 1				Scanner 2				Scanner 3				Scanner 4				Scanner 5				Scanner 6			
		Cor	Ax	Sag	\overline{ADC}	Cor	Ax	Sag	\overline{ADC}	Cor	Ax	Sag	\overline{ADC}	Cor	Ax	Sag	\overline{ADC}	Cor	Ax	Sag	\overline{ADC}	Cor	Ax	Sag	\overline{ADC}
1	2.000	2.064	2.037	2.097	2.066	2.091	2.100	2.099	2.097	2.056	2.090	2.097	2.081	2.091	2.096	2.134	2.107	2.108	2.072	2.093	2.091	2.048	2.058	2.046	2.050
2	2.000	2.069	2.061	2.133	2.088	2.093	2.038	2.035	2.055	2.098	2.105	2.083	2.095	2.066	2.068	2.046	2.060	2.108	2.074	2.038	2.074	2.017	2.085	2.074	2.058
3	2.000	1.987	2.107	2.045	2.046	2.106	2.056	2.015	2.059	2.078	2.108	2.078	2.088	2.067	2.039	2.035	2.047	2.102	2.080	2.054	2.079	2.003	2.113	2.054	2.056
4	1.551	1.590	1.563	1.563	1.572	1.601	1.596	1.579	1.592	1.564	1.623	1.592	1.593	1.603	1.560	1.559	1.574	1.606	1.581	1.555	1.581	1.591	1.605	1.572	1.589
5	1.551	1.508	1.536	1.586	1.544	1.598	1.623	1.579	1.600	1.555	1.617	1.584	1.585	1.616	1.651	1.526	1.598	1.595	1.597	1.548	1.580	1.590	1.617	1.555	1.587
6	1.183	1.171	1.172	1.187	1.176	1.154	1.196	1.208	1.186	1.178	1.185	1.155	1.172	1.202	1.223	1.176	1.200	1.193	1.176	1.162	1.177	1.196	1.183	1.164	1.181
7	1.183	1.167	1.158	1.208	1.177	1.130	1.233	1.225	1.196	1.189	1.187	1.134	1.170	1.162	1.276	1.232	1.223	1.186	1.201	1.161	1.183	1.197	1.205	1.170	1.191
8	0.832	0.818	0.855	0.823	0.832	0.817	0.843	0.839	0.833	0.824	0.811	0.820	0.818	0.841	0.817	0.898	0.852	0.853	0.828	0.824	0.835	0.821	0.822	0.799	0.814
9	0.832	0.757	0.854	0.811	0.807	0.835	0.860	0.834	0.843	0.790	0.827	0.829	0.815	0.847	0.856	0.918	0.874	0.818	0.839	0.831	0.829	0.801	0.833	0.767	0.800
10	0.507	0.512	0.577	0.490	0.526	0.541	0.537	0.544	0.541	0.533	0.535	0.535	0.534	0.582	0.489	0.573	0.548	0.543	0.536	0.531	0.537	0.533	0.536	0.502	0.524
11	0.507	0.515	0.602	0.487	0.535	0.548	0.531	0.510	0.529	0.544	0.551	0.588	0.561	0.567	0.468	0.577	0.537	0.528	0.543	0.531	0.534	0.530	0.551	0.495	0.525
12	0.267	0.309	0.390	0.293	0.331	0.294	0.279	0.292	0.288	0.322	0.291	0.282	0.298	0.307	0.284	0.322	0.304	0.292	0.311	0.274	0.292	0.297	0.302	0.284	0.294
13	0.267	0.289	0.383	0.308	0.327	0.296	0.278	0.290	0.288	0.320	0.305	0.287	0.304	0.292	0.315	0.267	0.291	0.297	0.308	0.294	0.300	0.304	0.309	0.311	0.308

3T ADC x 10⁻³ [mm²/s]

ROI	Ref	Scanner 7				Scanner 8				Scanner 9				Scanner 10				Scanner 11				Scanner 12			
		Cor	Ax	Sag	\overline{ADC}	Cor	Ax	Sag	\overline{ADC}	Cor	Ax	Sag	\overline{ADC}	Cor	Ax	Sag	\overline{ADC}	Cor	Ax	Sag	\overline{ADC}	Cor	Ax	Sag	\overline{ADC}
1	2.000	2.006	2.019	1.995	2.007	2.012	2.010	1.999	2.007	1.964	2.010	1.982	1.985	1.991	2.003	2.013	2.002	2.043	2.042	2.063	2.049	2.000	1.979	1.984	1.988
2	2.000	2.027	2.062	2.050	2.046	2.005	2.039	2.035	2.026	1.975	2.018	1.947	1.980	1.991	2.034	2.025	2.016	2.022	2.010	2.024	2.019	2.021	2.013	2.008	2.014
3	2.000	1.985	2.113	2.043	2.047	1.967	2.075	2.089	2.043	1.950	2.044	1.967	1.987	2.035	2.032	1.966	2.011	2.046	2.032	1.951	2.001	2.014	2.057	1.987	2.019
4	1.551	1.552	1.644	1.530	1.575	1.527	1.588	1.584	1.566	1.509	1.570	1.549	1.543	1.562	1.564	1.549	1.558	1.589	1.597	1.569	1.585	1.549	1.563	1.536	1.549
5	1.551	1.523	1.662	1.488	1.558	1.517	1.619	1.563	1.567	1.491	1.593	1.582	1.556	1.568	1.587	1.546	1.567	1.592	1.619	1.534	1.582	1.535	1.595	1.484	1.538
6	1.183	1.193	1.193	1.213	1.200	1.169	1.188	1.143	1.167	1.141	1.172	1.158	1.157	1.166	1.172	1.168	1.169	1.164	1.225	1.232	1.207	1.164	1.172	1.136	1.157
7	1.183	1.213	1.127	1.198	1.179	1.195	1.196	1.108	1.166	1.163	1.182	1.136	1.160	1.139	1.179	1.187	1.168	1.145	1.210	1.166	1.174	1.198	1.188	1.174	1.186
8	0.832	0.848	0.794	0.838	0.827	0.829	0.827	0.806	0.821	0.792	0.851	0.796	0.813	0.805	0.810	0.794	0.803	0.824	0.869	0.826	0.840	0.818	0.820	0.814	0.817
9	0.832	0.814	0.812	0.807	0.811	0.813	0.830	0.814	0.819	0.770	0.829	0.804	0.801	0.842	0.829	0.795	0.822	0.833	0.820	0.886	0.846	0.824	0.833	0.799	0.819
10	0.507	0.554	0.524	0.563	0.547	0.523	0.546	0.539	0.536	0.502	0.537	0.520	0.520	0.529	0.532	0.516	0.525	0.545	0.569	0.568	0.560	0.527	0.549	0.524	0.533
11	0.507	0.519	0.513	0.557	0.530	0.525	0.534	0.539	0.532	0.494	0.548	0.531	0.524	0.535	0.486	0.540	0.520	0.533	0.536	0.533	0.534	0.528	0.526	0.532	0.528
12	0.267	0.313	0.345	0.329	0.329	0.293	0.287	0.295	0.291	0.283	0.299	0.283	0.288	0.290	0.293	0.299	0.294	0.295	0.294	0.306	0.298	0.299	0.288	0.290	0.292
13	0.267	0.308	0.329	0.324	0.320	0.304	0.298	0.294	0.298	0.301	0.303	0.277	0.294	0.280	0.317	0.316	0.304	0.283	0.274	0.289	0.282	0.308	0.291	0.306	0.302

Ref = reference; Cor = coronal; Ax = axial; Sag = sagittal

Table S4: Accuracy error% for each vial and scanner

Accuracy Error% 1.5T

ROI	Ref	Scanner 1			Scanner 2			Scanner 3			Scanner 4			Scanner 5			Scanner 6									
		Cor	Ax	Sag	\overline{ADC}	Cor	Ax	Sag	\overline{ADC}	Cor	Ax	Sag	\overline{ADC}	Cor	Ax	Sag	\overline{ADC}	Cor	Ax	Sag	\overline{ADC}					
1	2.000	3.21	1.87	4.84	3.31	4.53	4.99	4.96	4.83	2.80	4.49	4.85	4.05	4.56	4.79	6.71	5.35	5.42	3.62	4.66	4.57	2.40	2.89	2.29	2.52	..
2	2.000	3.44	3.05	6.64	4.38	4.67	1.89	1.76	2.77	4.91	5.26	4.13	4.77	3.32	3.40	2.32	3.01	5.41	3.72	1.89	3.67	0.85	4.25	3.70	2.93	.
3	2.000	0.66	5.36	2.24	2.31	5.31	2.79	0.77	2.96	3.88	5.40	3.90	4.39	3.37	1.93	1.73	2.34	5.09	4.02	2.73	3.95	0.17	5.67	2.70	2.84	.
4	1.551	2.53	0.75	0.78	1.35	3.20	2.93	1.82	2.65	0.84	4.61	2.61	2.69	3.35	0.57	0.53	1.48	3.56	1.94	0.22	1.91	2.59	3.50	1.32	2.47	.
5	1.551	2.75	0.94	2.27	0.47	3.03	4.67	1.83	3.18	0.27	4.22	2.11	2.20	4.20	6.44	1.58	3.02	2.83	2.96	0.22	1.85	2.51	4.28	0.25	2.35	.
6	1.183	1.05	0.94	0.33	0.56	2.45	1.11	2.11	0.26	0.46	0.15	2.37	0.89	1.62	3.38	0.62	1.46	0.91	0.59	1.76	0.48	1.07	0.04	1.61	0.17	.
7	1.183	1.34	2.15	2.08	0.47	4.45	4.21	3.58	1.11	0.49	0.34	4.14	1.11	1.76	7.85	4.11	3.40	0.26	1.58	1.84	0.00	1.20	1.83	1.12	0.64	.
8	0.832	1.74	2.78	1.12	0.03	1.80	1.27	0.85	0.11	1.02	2.52	1.50	1.68	1.10	1.75	7.88	2.40	2.55	0.53	1.00	0.34	1.27	1.21	3.91	2.13	.
9	0.832	9.05	2.69	2.51	2.95	0.37	3.34	0.19	1.30	5.08	0.66	0.36	2.03	1.83	2.86	10.35	5.01	1.65	0.89	0.18	0.31	3.67	0.14	7.87	3.80	.
10	0.507	0.95	13.74	3.36	3.78	6.67	5.98	7.31	6.65	5.13	5.42	5.42	5.33	14.86	3.51	12.94	8.09	7.12	5.80	4.83	5.91	5.15	5.64	0.90	3.30	.
11	0.507	1.49	18.68	3.89	5.43	8.00	4.70	0.58	4.42	7.20	8.63	15.93	10.59	11.83	7.70	13.90	6.01	4.20	7.15	4.64	5.33	4.46	8.74	2.43	3.59	.
12	0.267	15.73	46.15	9.86	23.91	9.93	4.32	9.45	7.90	20.41	8.99	5.71	11.70	15.01	6.20	20.63	13.94	9.68	16.55	2.62	9.62	11.32	13.28	6.18	10.26	.
13	0.267	8.31	43.58	15.27	22.39	10.87	4.17	8.58	7.87	19.76	14.04	7.30	13.70	9.34	18.00	0.07	9.10	11.24	15.45	10.32	12.34	13.75	15.71	16.46	15.31	.

Accuracy Error% 3T

ROI	Ref	Scanner 7			Scanner 8			Scanner 9			Scanner 10			Scanner 11			Scanner 12									
		Cor	Ax	Sag	\overline{ADC}	Cor	Ax	Sag	\overline{ADC}	Cor	Ax	Sag	\overline{ADC}	Cor	Ax	Sag	\overline{ADC}	Cor	Ax	Sag	\overline{ADC}					
1	2.000	0.28	0.94	0.24	0.33	0.58	0.51	0.03	0.35	1.80	0.48	0.91	0.74	0.45	0.12	0.63	0.10	2.13	2.10	3.14	2.46	0.00	1.05	0.80	0.62	.
2	2.000	1.37	3.07	2.51	2.32	0.24	1.93	1.77	1.31	1.26	0.90	2.64	1.00	0.46	1.68	1.25	0.82	1.11	0.48	1.22	0.93	1.06	0.66	0.41	0.71	.
3	2.000	0.76	5.65	2.17	2.35	1.67	3.75	4.45	2.17	2.49	2.21	1.64	0.64	1.76	1.57	1.68	0.55	2.31	1.61	2.43	0.50	0.68	2.84	0.63	0.96	.
4	1.551	0.05	5.96	1.34	1.55	1.58	2.41	2.12	0.98	2.68	1.19	0.11	0.53	0.68	0.84	0.15	0.45	2.46	2.94	1.16	2.18	0.16	0.79	1.00	0.12	.
5	1.551	1.85	7.16	4.04	0.42	2.17	4.40	0.77	1.00	3.84	2.71	2.02	0.30	1.11	2.32	0.32	1.04	2.67	4.40	1.13	1.98	1.03	2.84	4.29	0.83	.
6	1.183	0.83	0.87	2.51	1.40	1.22	0.44	3.35	1.38	3.53	0.96	2.14	2.21	1.44	0.97	1.27	1.23	1.65	3.51	4.18	2.01	1.59	0.94	4.00	2.18	.
7	1.183	2.51	4.72	1.26	0.31	1.00	1.08	6.35	1.42	1.72	0.10	3.97	1.93	3.74	0.34	0.31	1.26	3.19	2.26	1.40	0.77	1.26	0.38	0.78	0.29	.
8	0.832	1.89	4.59	0.77	0.64	0.33	0.64	3.15	1.38	4.81	2.27	4.30	2.28	3.31	2.64	4.61	3.52	0.96	4.39	0.69	0.91	1.73	1.50	2.18	1.80	.
9	0.832	2.23	2.41	2.97	2.54	2.31	0.22	2.14	1.56	7.45	0.33	3.36	3.71	1.17	0.36	4.49	1.23	0.11	1.40	6.51	1.74	1.00	0.12	3.94	1.61	.
10	0.507	9.15	3.30	11.07	7.83	3.06	7.61	6.32	5.66	0.99	5.94	2.61	2.52	4.34	4.83	1.71	3.63	7.45	12.19	11.99	10.54	4.04	8.19	3.36	5.19	.
11	0.507	2.24	1.18	9.87	4.43	3.47	5.27	6.23	4.99	2.56	8.07	4.79	3.43	5.47	4.24	6.44	2.56	5.22	5.80	5.22	5.42	4.08	3.75	4.86	4.23	.
12	0.267	16.96	29.00	23.35	23.10	9.62	7.39	10.39	9.13	6.09	11.89	6.01	8.00	8.52	9.74	11.99	10.08	10.45	10.08	14.47	11.67	11.80	7.88	8.80	9.49	.
13	0.267	15.32	23.25	21.43	20.00	13.74	11.42	9.96	11.71	12.84	13.36	3.67	9.96	4.78	18.54	18.48	13.93	6.15	2.77	8.25	5.73	15.27	9.16	14.45	12.96	.

Ref = reference, Cor = coronal; Ax = axial; Sag = sagittal

Table S5: Summary of GLMM statistical significance of predictors for accuracy, repeatability and precision. Field and vendor were tested as independent predictors and through their interaction for each variable.

	<i>Field</i>	<i>Vendor</i>	<i>Field x vendor</i>
Accuracy (coronal)	0.02991 *	0.26751	0.8140
Accuracy (axial)	0.001738 **	0.011627 *	0.457170
Accuracy (sagittal)	0.5407	0.1730	0.15771
Accuracy (average)	0.005367 **	0.258755	0.66136
Repeatability (coronal)	4.287e-15 ***	1.708e-07 ***	0.02821 *
Repeatability (axial)	7.489e-11 ***	8.570e-11 ***	1.959e-06 ***
Repeatability (sagittal)	0.02141 *	0.16935	0.81516
Precision (coronal)	0.03889 *	0.00770 **	0.01697 *
Precision (axial)	0.2883	5.378e-07 ***	0.11579
Precision (sagittal)	0.1792	0.3850	0.30970
Precision (average)	0.122983	0.007146 **	0.097245

* = p<0.05, ** p <0.01, *** = p<0.001

Table S6: Intra-session coefficient of variation ($CV_{\text{intra}}\%$) for each vial and scanner

$CV_{\text{intra}}\% 1.5T$																		
ROI	Scanner 1			Scanner 2			Scanner 3			Scanner 4			Scanner 5			Scanner 6		
	Cor	Ax	Sag	Cor	Ax	Sag	Cor	Ax	Sag	Cor	Ax	Sag	Cor	Ax	Sag	Cor	Ax	Sag
1	1.31	0.76	0.88	0.18	0.48	0.55	0.18	0.18	0.21	0.48	0.46	0.78	0.40	0.23	0.98	0.27	0.42	1.31
2	0.51	0.87	0.47	0.30	0.33	0.37	0.29	0.26	0.18	0.42	0.31	0.71	0.31	0.23	0.82	0.23	0.40	0.51
3	0.60	0.19	1.88	0.70	0.15	0.35	0.42	0.31	0.17	0.34	0.17	0.17	0.42	0.56	0.37	0.43	0.40	0.60
4	1.35	0.60	1.21	0.57	0.28	0.39	0.16	0.12	0.11	0.37	1.69	0.18	0.15	0.26	1.44	0.62	0.35	1.35
5	0.34	0.93	0.85	0.30	0.22	0.29	0.40	0.12	0.11	0.39	0.72	0.41	0.68	0.39	1.01	0.14	0.20	0.34
6	0.60	1.81	1.07	0.16	0.17	0.66	0.53	0.19	0.31	1.04	0.86	0.18	0.36	0.12	0.12	0.49	0.28	0.60
7	1.06	0.40	0.21	0.13	0.22	0.34	0.19	0.18	0.51	0.81	0.78	0.05	0.32	0.52	0.23	0.30	0.40	1.06
8	1.21	0.64	1.89	0.25	0.13	0.67	0.64	0.51	0.37	0.92	1.88	1.79	0.85	1.10	1.37	0.14	0.12	1.21
9	0.82	0.47	0.35	0.79	0.67	0.20	0.51	0.25	0.38	0.89	0.34	1.21	0.67	0.08	0.85	0.32	0.43	0.82
10	1.28	1.75	0.44	0.75	0.74	0.60	0.88	0.45	1.31	1.74	1.22	0.48	0.62	0.52	0.77	0.72	0.18	1.28
11	0.82	1.10	3.14	1.13	0.25	0.80	0.44	0.45	1.20	1.31	2.26	0.48	0.31	0.50	0.91	0.09	0.31	0.82
12	5.47	1.27	2.99	0.95	1.41	1.11	0.82	1.09	0.61	1.22	4.84	2.46	1.28	1.12	1.19	0.47	0.73	5.47
13	4.72	2.15	5.48	0.27	0.61	0.92	0.54	1.48	1.09	0.38	1.16	1.03	0.99	1.35	0.70	1.66	1.38	4.72
$CV_{\text{intra}}\% 3T$																		
ROI	Scanner 7			Scanner 8			Scanner 9			Scanner 10			Scanner 11			Scanner 12		
	Cor	Ax	Sag	Cor	Ax	Sag	Cor	Ax	Sag	Cor	Ax	Sag	Cor	Ax	Sag	Cor	Ax	Sag
1	0.27	0.12	0.09	0.10	0.10	0.18	0.12	0.12	0.26	0.30	0.11	0.15	0.09	0.65	0.03	0.09	0.29	0.22
2	0.08	0.42	0.09	0.20	0.29	0.09	0.15	0.11	0.05	0.23	0.17	0.69	0.06	0.28	0.38	0.27	0.26	0.14
3	0.29	0.13	0.14	0.14	0.17	0.16	0.27	0.23	0.06	0.38	0.45	0.85	0.25	0.20	0.22	0.17	0.47	0.34
4	0.10	0.18	0.08	0.04	0.11	0.12	0.17	0.28	0.03	0.28	0.18	0.48	0.13	0.09	0.09	0.07	0.46	0.17
5	0.12	0.36	0.13	0.14	0.17	0.16	0.15	0.52	0.12	0.31	0.45	0.51	0.29	0.09	0.14	0.19	0.16	0.15
6	0.11	0.28	0.21	0.18	0.21	0.17	0.05	0.27	0.04	0.43	0.54	0.68	0.13	0.18	0.35	0.11	0.41	0.18
7	0.10	0.76	0.25	0.20	0.19	0.10	0.31	0.45	0.18	0.18	0.24	0.51	0.13	0.75	0.40	0.23	0.11	0.28
8	0.58	0.37	0.18	0.24	0.30	0.19	0.11	0.56	0.15	0.30	0.17	1.34	0.20	1.07	0.08	0.20	0.11	0.17
9	0.28	0.35	0.14	0.12	0.32	0.19	0.25	0.67	0.12	0.26	0.68	1.05	0.28	0.57	0.09	0.56	0.63	0.56
10	0.17	0.65	0.17	0.55	0.95	1.70	0.32	0.14	0.39	0.27	0.13	0.62	0.10	0.37	0.26	0.15	0.86	0.47
11	0.19	0.60	0.35	0.62	0.86	0.47	1.04	0.41	0.62	0.41	0.44	1.26	0.15	0.40	0.42	0.28	0.18	0.18

12	0.74	0.37	0.24	0.26	0.32	1.69	0.62	0.39	0.41	0.71	0.48	1.34	0.41	1.36	0.73	0.19	0.17	0.57
13	0.68	0.61	0.15	0.25	0.81	1.28	0.25	0.31	0.88	0.34	0.22	1.80	0.58	0.47	0.28	0.68	1.07	0.16

Cor = coronal; Ax = axial; Sag = sagittal

Figure S6: GLMM results for accuracy error (in %) compared across slice orientations in the full range (a) and reduced range (b). Horizontal lines represent the paired comparisons with their relative Bonferroni-corrected significance value (ns = $p > 0.05$, * = $p < 0.05$, ** $p < 0.01$, *** = $p < 0.001$).

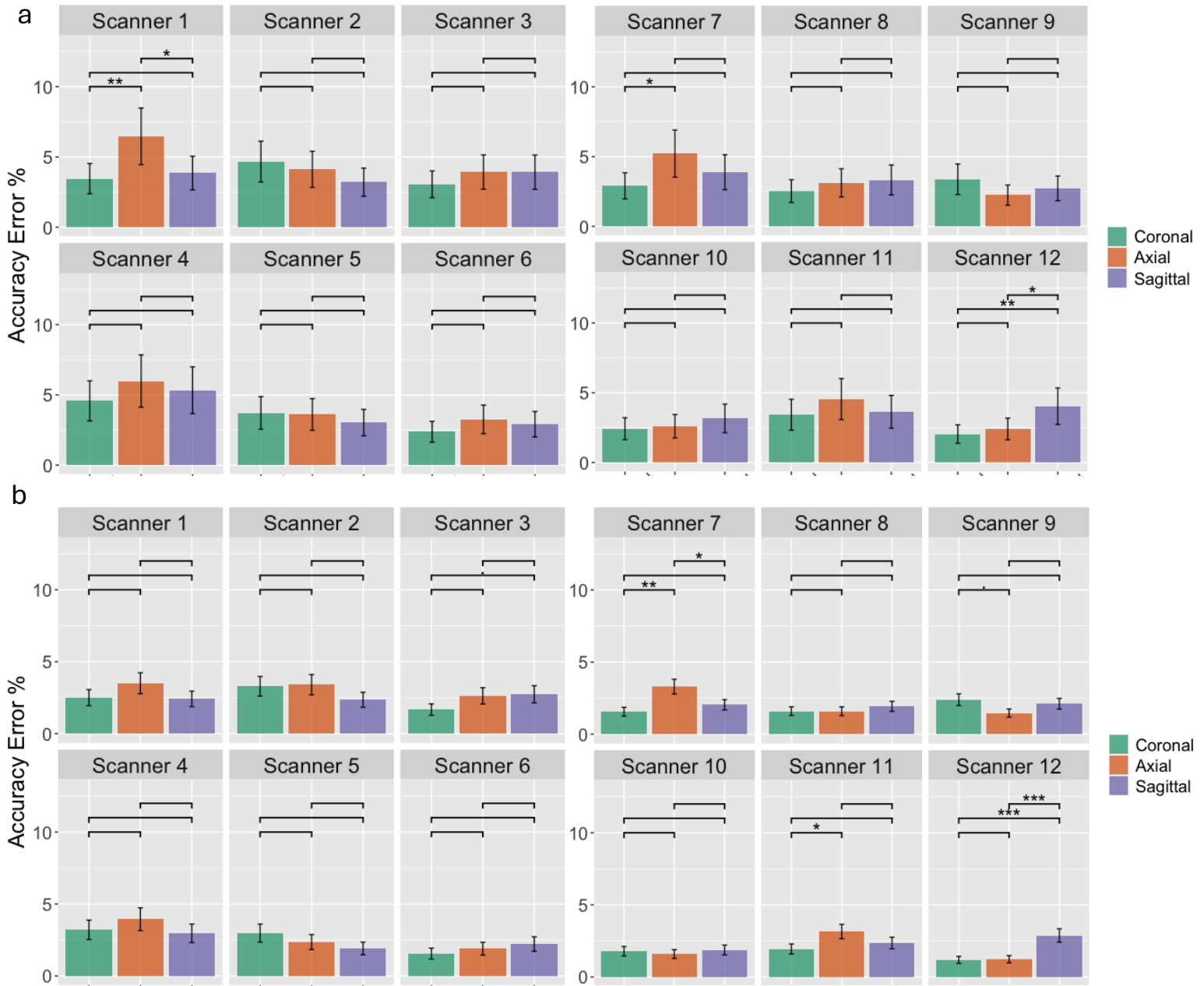
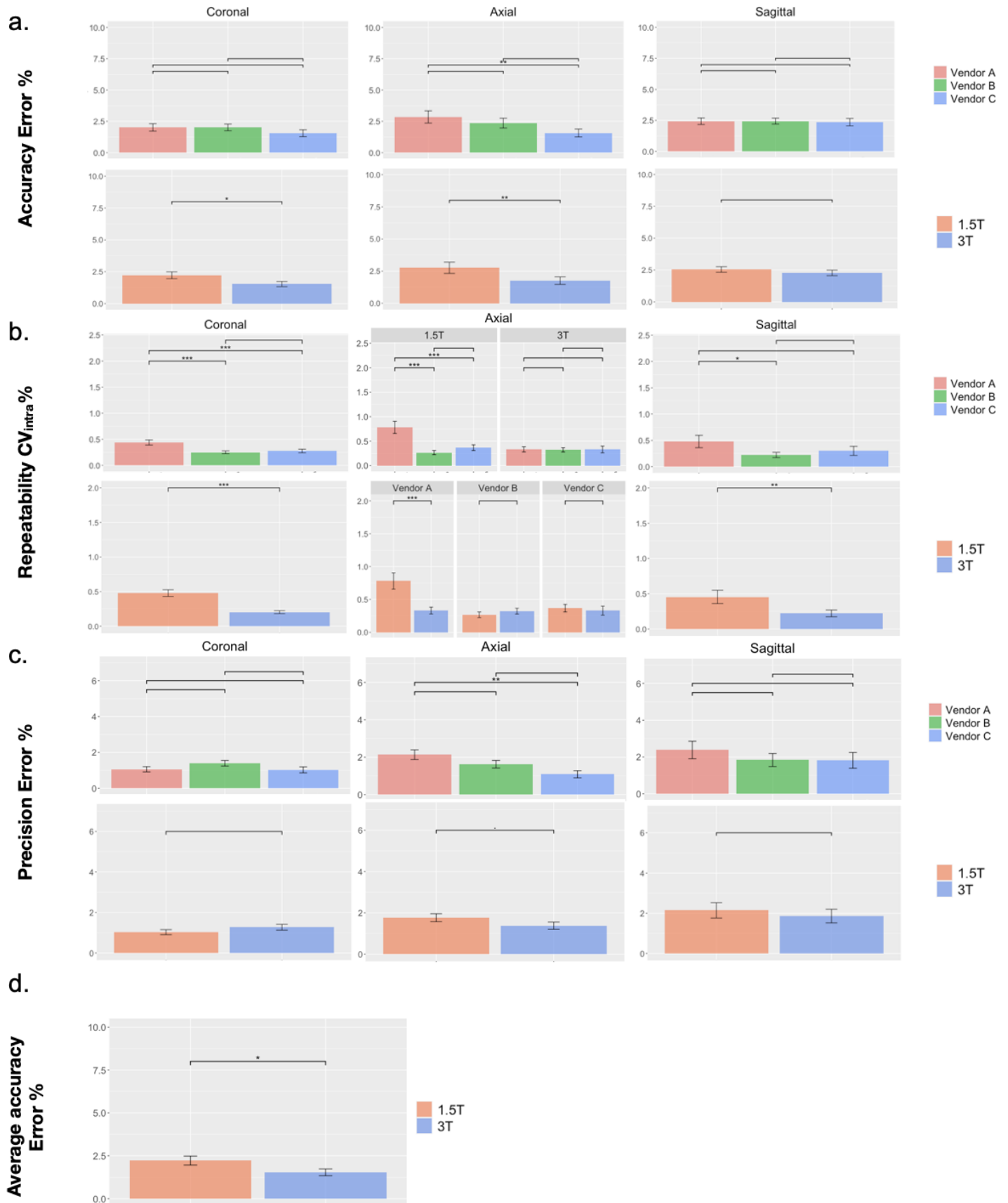


Figure S7: Results of GLMM in the reduced range on accuracy error (a), repeatability (b) and precision error (c) across all imaging planes. Accuracy error is also reported for average values (d). All results are reported as least-square means and standard errors. Horizontal lines represent the paired comparisons with their relative Bonferroni-corrected significance value (ns = $p > 0.05$, * = $p < 0.05$, ** $p < 0.01$, *** = $p < 0.001$).



In the reduced range for coronal and sagittal direction field and vendor are significant independent predictors for $CV_{intra}\%$ while for axial direction their interaction is significant ($p=2.31 \times 10^{-4}$); furthermore, average precision error had no significant independent predictor thus no significant differences were found between 1.5T and 3T scanners and among vendors.

Figure S8: GLMM results for intra-session coefficient of variation ($CV_{intra}\%$) compared across slice orientations in the full range (a) and reduced range (b). Horizontal lines represent the paired comparisons with their relative Bonferroni-corrected significance value (ns = $p > 0.05$, * = $p < 0.05$, ** $p < 0.01$, *** = $p < 0.001$).

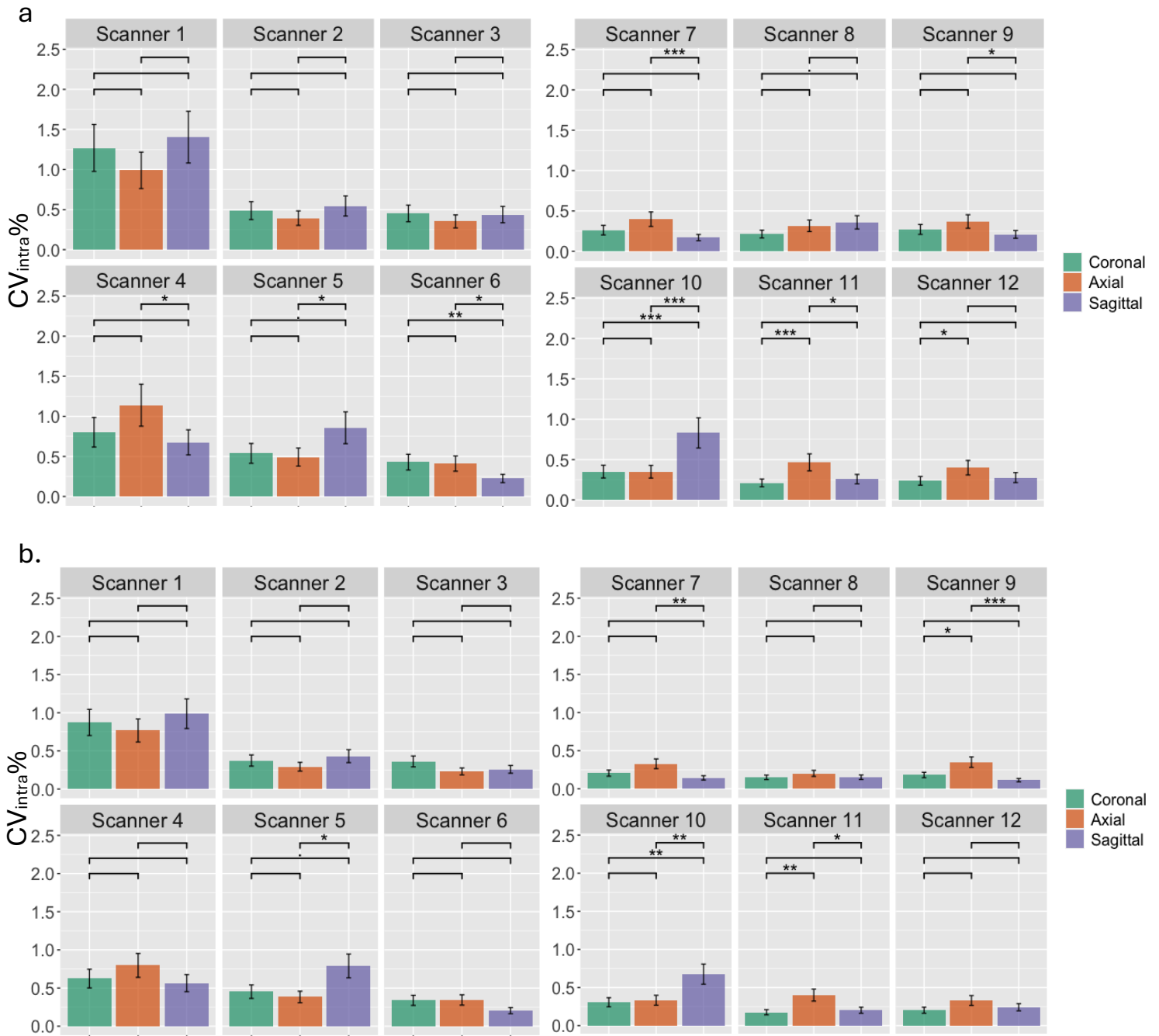
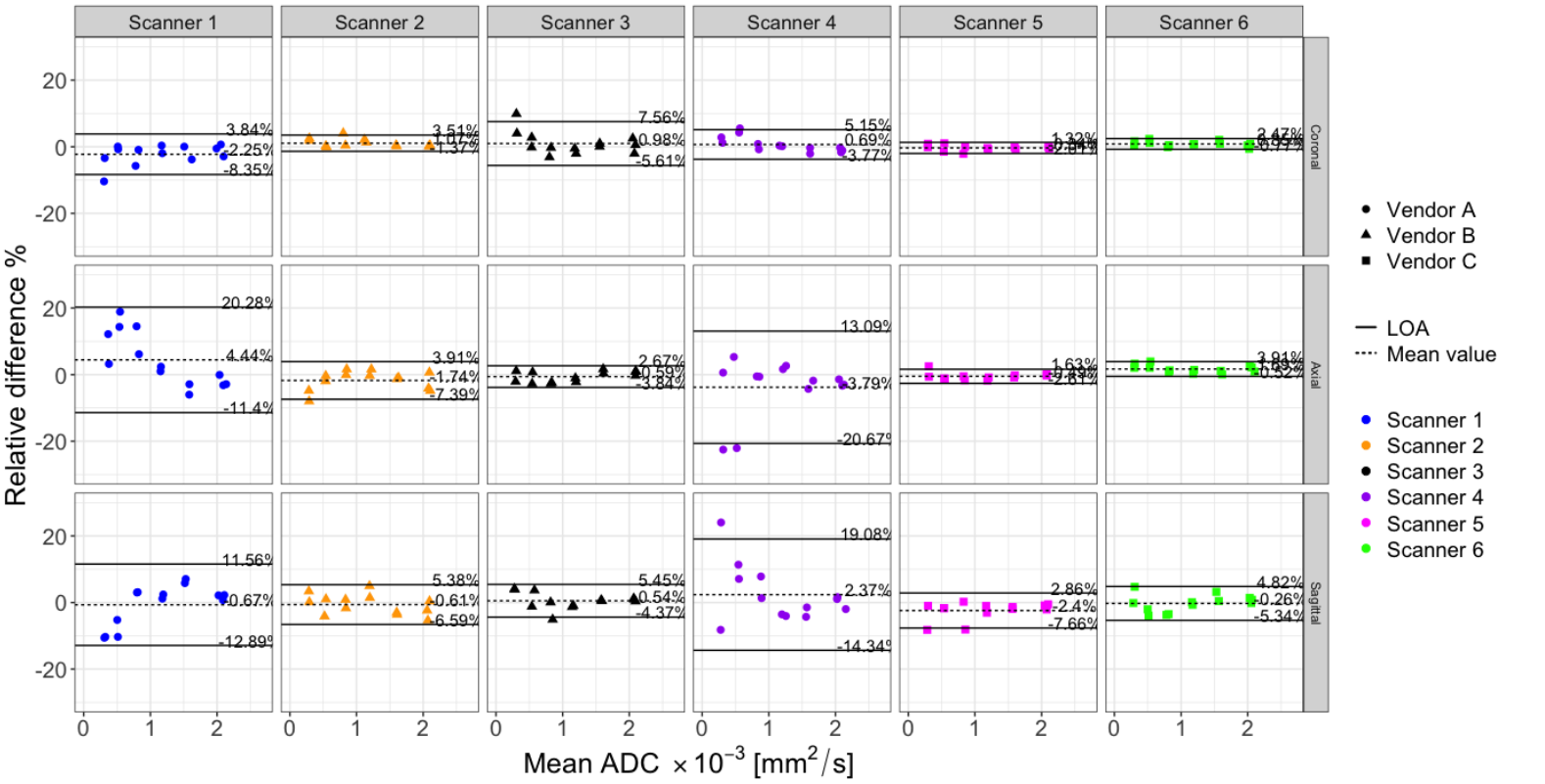


Figure S9: Bland Altman plots for test-retest measurements across each imaging slice orientation

1.5T



3T

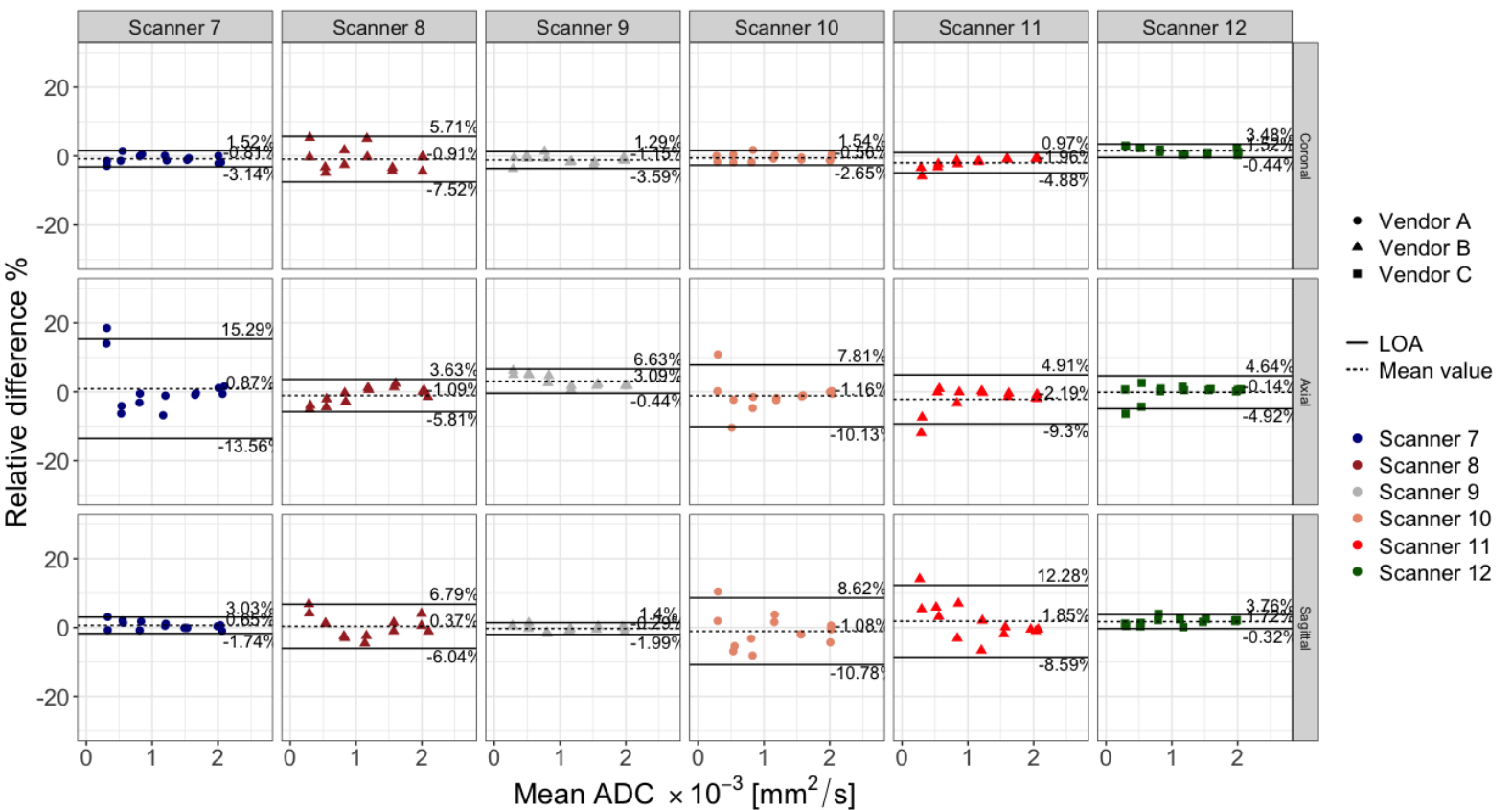


Figure S10: GLMM results for precision error% compared across slice orientations in the full range (a) and reduced range (b). . Horizontal lines represent the paired comparisons with their relative Bonferroni-corrected significance value (ns = $p > 0.05$, * = $p < 0.05$, ** $p < 0.01$, *** = $p < 0.001$).

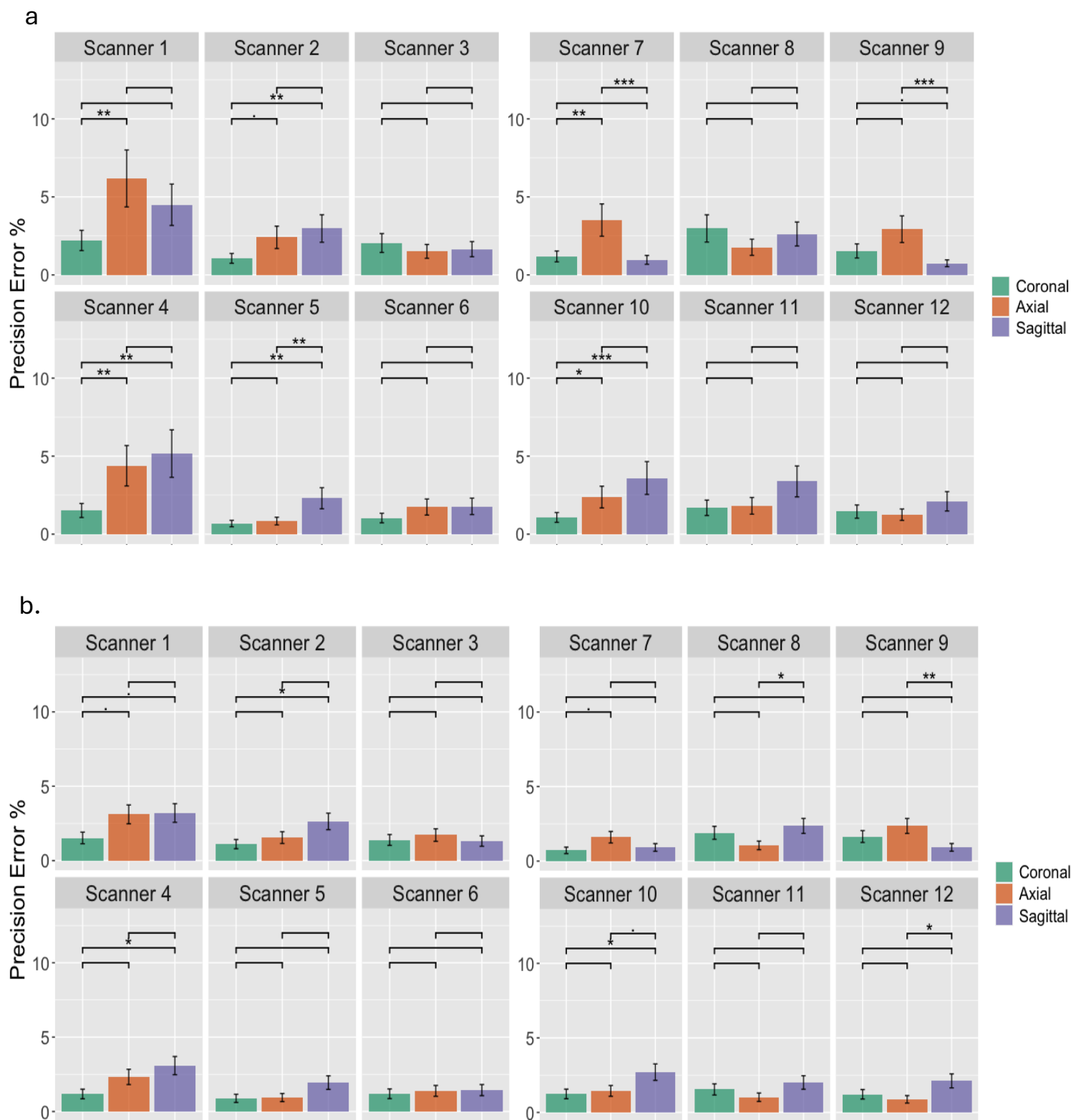


Table S7: Results of ADC variance contributions, ICC_{intra} and ICC_{inter} are reported for both field strengths

	1.5T		3T	
	ICC _{intra}	ICC _{inter}	ICC _{intra}	ICC _{inter}
ROI-1	0.134	0.866	0.049	0.951
ROI-2	0.350	0.650	0.146	0.854
ROI-3	0.472	0.528	0.223	0.777
ROI-4	0.587	0.413	0.126	0.874
ROI-5	0.148	0.852	0.114	0.886
ROI-6	0.198	0.802	0.032	0.968
ROI-7	0.231	0.769	0.306	0.694
ROI-8	0.360	0.640	0.225	0.775
ROI-9	0.117	0.883	0.179	0.821
ROI-10	0.464	0.536	0.117	0.883
ROI-11	0.232	0.768	0.533	0.467
ROI-12	0.048	0.952	0.206	0.794
ROI-13	0.081	0.919	0.242	0.758

ICC_{intra} = intra-class correlation coefficient; ICC_{inter} inter-class correlation coefficient

Overall ICC_{inter} was greater than ICC_{intra} however there were some exceptions for which ICC values were close to the ideal value of 0.5. This was true for ICC calculated on 1.5T scanners for ROI-3, ROI-4 and ROI-9 and on 3T scanners for ROI-11.